Experimental study of the combustion properties of methane/hydrogen mixtures

Gersen, Sander

Chapter 5

Extractive Probe Measurements of Acetylene in Atmospheric-Pressure Fuel-Rich Premixed Methane/Air Flames

5.1 Introduction

As discussed in previous chapters, one of the major advances of the last decades in the combustion science is the prediction of flame structure by numerical simulations using detailed transport and chemical mechanisms. Because of the complexity of these mechanisms and uncertainties in the rates of the key chemical reactions, the predictive power of the numerical simulations can be tested only by comparing calculated and measured flame properties under well-defined experimental conditions. The comparison of the spatial profiles of intermediate species is particularly important for testing the adequacy of chemical mechanisms. One of the key intermediates in many high temperature processes is acetylene (C_2H_2), which plays important role in the formation of polycyclic aromatic hydrocarbons and soot in hydrocarbon combustion [1-3] and in the chemical vapor deposition of diamond [4].

Acetylene has been extensively investigated in both atmospheric- and low-pressure flat premixed flames [5-11]. At atmospheric pressure, large discrepancies have been observed [8,11] between measured results and those calculated based on the C_2H_2 submechanism derived from Miller and Mellius [12]. However, the acetylene measurements in these studies were performed using extractive probe sampling, which as discussed in Chapter 4 has a serious drawback, i.e., the distortion of the composition and temperature profiles in the flame. Estimating the magnitude of this distortion, for example, from chemical reactions on the probe surface or acceleration of the combustion products into the probe orifice are rather difficult [13]. Moreover, these estimates (as was done in Chapter 4) require detailed knowledge of the kinetics of the chemical reactions involving the measured species that itself is the subject of investigation. These complications necessitate the verification of the results obtained by the extractive probe by an independent technique. Recently, we have reported the measurement of native C_2H_2 in a fuel-rich methane/air flame at equivalence ratio $\varphi = 1.55$, using spontaneous Raman scattering [14]. This method thus provides us with the means to verify the results of extractive probe sampling for acetylene measurement, and to deliver reliable experimental results regarding C_2H_2 formation and destruction in atmospheric-pressure methane/air flames.

Towards this end, we have measured the profiles of C_2H_2 mole fraction in flat atmospheric-pressure rich-premixed methane/air flames using both spontaneous Raman scattering and microprobe gas sampling followed by tunable diode laser

absorption spectroscopy (TDLAS). These measurements are supplemented with profiles of flame temperature, obtained using coherent anti-Stokes Raman Scattering (CARS), and the experimental results are compared with the predictions of one-dimensional flame calculations.

5.2 Experimental

Here we briefly summarize the experimental method; Chapter 4 discusses the methods in more detail. The measurements were performed in atmospheric-pressure methane/air flames stabilized above a McKenna Products sintered bronze burner of 60 mm diameter. To prevent air entrainment in the combustion products a nitrogen shroud was used. The flame was stabilized by a cylindrical chimney with a 60 mm inner diameter, which was positioned approximately 30 mm above the burner surface. The flame temperature was varied by changing the mass flow through the burner and measured by broadband planar BOXCARS for nitrogen thermometry. Details of the CARS experiment are described elsewhere [15]. The flow rates of methane and air were measured by calibrated mass flow meters and the equivalence ratio was determined by measuring the methane concentration in the unburned fuel-air mixture. For calibration purposes, nitrogen doped with a known amount of acetylene was flowed through the burner instead of the methane-air mixture. Measurements were obtained at different axial positions in the flame by moving the burner with a precision positioner relative to the laser beams and sampling probe in steps of 1 mm. The flames were sampled by a cooled quartz micro-probe, and the sampled gas flowed through an absorption cell and analyzed using TDLAS. As discussed in Chapter 4, estimates of C_2H_2 conversion during sampling indicated that in the present experimental setup conversion of acetylene in the probe is less than 15% when sampling is made at axial distances greater than 2.5 mm from the burner surface. These estimates are supported by measurements at different suction backpressures, which showed no significant changing in the measured HCN concentration when varying pressure from 0.05 to 0.35 Bar.

5.3 Results and discussion

The measurements were performed in a set of fuel-rich flames with different equivalence ratios and mass fluxes. The flame parameters (equivalence ratios, mass fluxes and temperatures at 5 mm above the burner surface) are presented in Table 5.1.

Table. 5.1. Flame parameters

Flame	φ	ρv, g/cm^2·s)	T, K
A	1.5	0.005	1763
B	1.5	0.007	1835
C	1.5	0.008	1852
D	1.45	0.007	1833
E	1.45	0.0085	1885
F	1.45	0.010	1916
G	1.4	0.005	1762
H	1.4	0.007	1816
I	1.4	0.0085	1850

The temperature measurements showed that all the flames studied had a domain with constant temperature extending at least 20 mm radially from the centerline, and from 3 mm to 15 mm in the axial direction. As typical examples of the temperature measurements, the radial profile at height 10 mm above the burner surface and centerline axial profile in flame A are presented in Figs. 5.1 and 5.2, respectively. The radial profile shows a core region of ~ 20 mm length of constant temperature surrounded by a layer where the temperature is higher due to penetrating surrounding air through the nitrogen shroud. The axial centerline temperature profile is in excellent agreement with the flame calculations, indicating the robustness of the GRI-Mech 3.0 [16] mechanism in predicting the burning velocities of CH_4/air flames and marginal radiative heat losses in these flames. The excellent agreement between measured and calculated axial temperature profiles was observed in all flames studied.

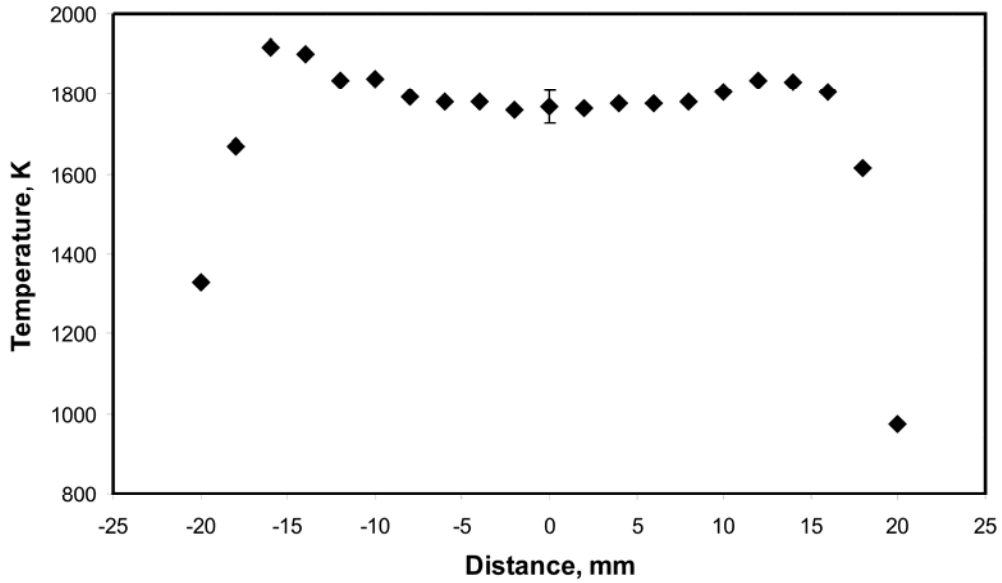

Figure 5.1. Radial temperature profile measured in flame A at 10 mm above the burner surface.

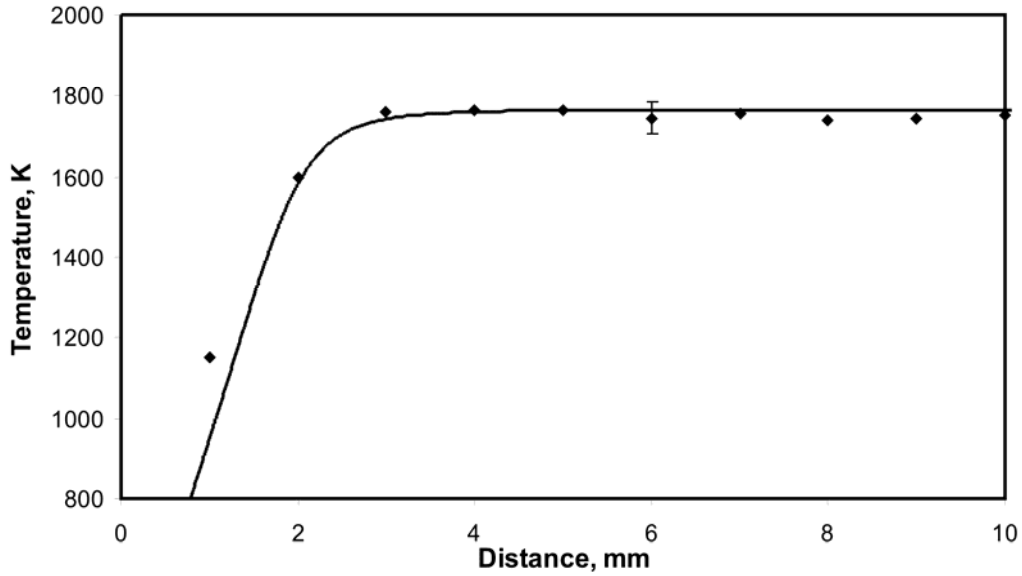

Figure 5.2. Axial centreline temperature profile measured in flame A. Solid line and diamonds denote flame calculations and measurements, respectively.

Acetylene mole fractions, measured by Raman scattering in flame C, and shown in figure 5.3, reach a maximum at an axial distance between 2 and 3 mm and then decrease to ~ 500 ppm at 9 mm, the detection limit of the current setup [15]. As can be seen in this figure, the profile obtained with the probe is shifted approximately 1.3 mm farther downstream. A similar shift between probe and optical measurements

was observed in temperature and hydroxyl profiles in other flames [17,18], and is the result of the acceleration of the combustion products into the probe orifice [13]. Shifting the probe profile results in agreement with the Raman profiles to better than 20% (also observed in Ref. [14] at φ = 1.58), which substantiates the extractive probe technique for the measurements of acetylene presented below.

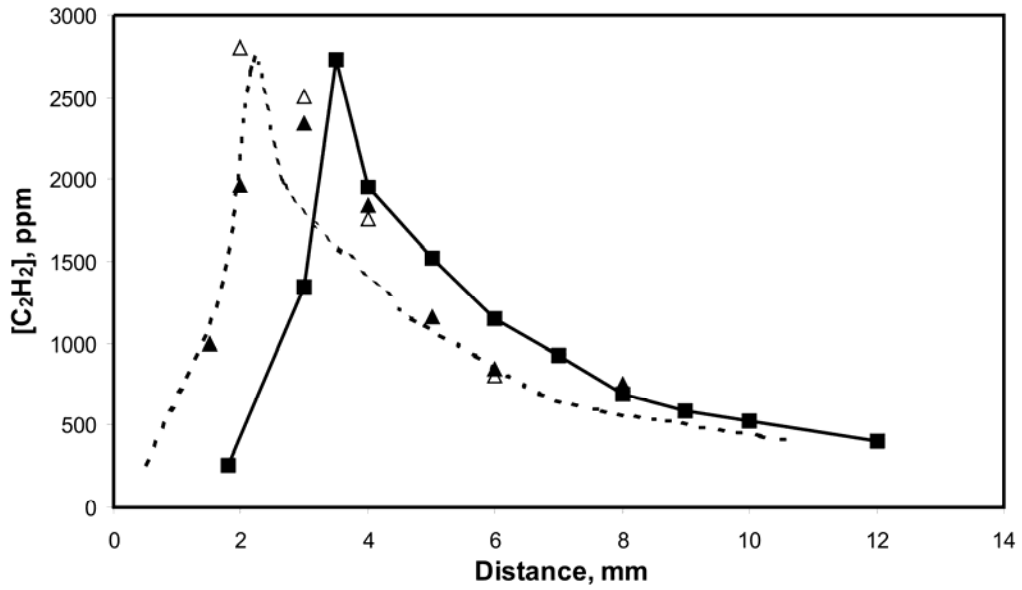

Figure 5.3. Axial centerline profiles of acetylene mole fraction in methane/air flame, φ = 1.50 and ρv = 0.008 g/(cm^2·s). Symbols denote Raman (triangles) and probe (squares with solid line) measurements; the dashed line denotes the shifted probe measurements.

At mole fractions below 500 ppm the acetylene Raman spectrum was barely distinguishable in the noise, while the signal-to-noise ratio of the TDLAS spectrum remained higher than 10 for mole fractions down to 100 ppm. This difference in the limit of detectability precludes comparison of probe and Raman data in the flames with low C_2H_2 mole fraction in the post-flame zone. However, due to the modest changes in flame structure upon changing the equivalence ratio from φ = 1.5 to φ = 1.4, we do not expect the accuracy of the probe measurements observed at φ = 1.58 and φ = 1.5 to deteriorate substantially. The results of the extractive probe measurements of acetylene at equivalence ratios φ = 1.5, 1.45 and 1.4 at different mass fluxes are presented in figure 5.4-5.6. Consistent with the results in figure 5.3 and those presented in Ref. [14], all experimental acetylene profiles are shifted

1.3 mm towards the burner surface. As can be seen from the figures, at a fixed equivalence ratio the maximum C_2H_2 mole fraction depends only slightly on the mass flux, while C_2H_2 oxidation in the post-flame zone increases substantially in the flames at higher the mass flux, caused by the higher gas temperatures (given in Table 5.1). At the same time, decreasing the equivalence ratio from $\varphi = 1.5$ to 1.4 decreases the peak C_2H_2 mole fraction by nearly a factor of two.

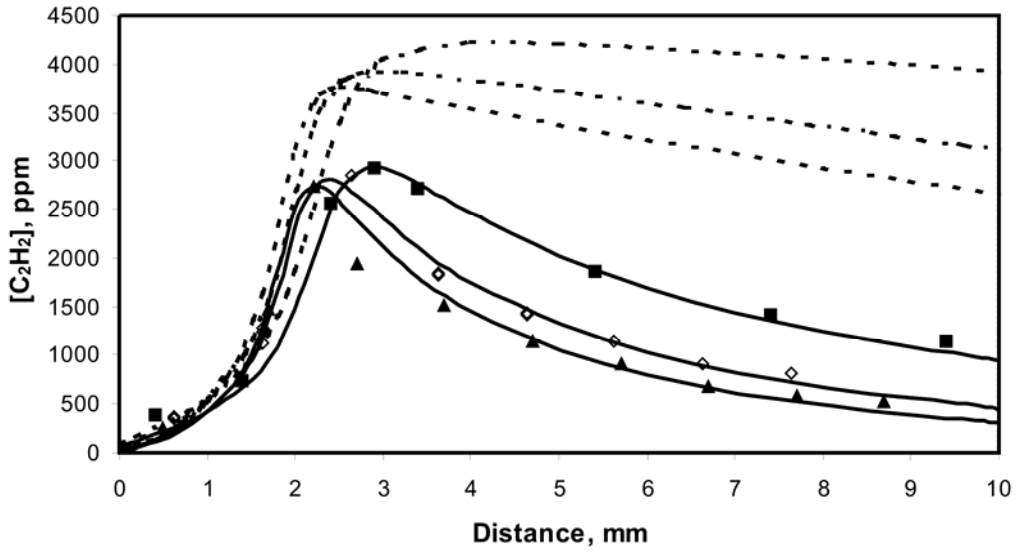

Figure 5.4. Axial profiles of acetylene mole fraction in methane/air flames, $\varphi = 1.5$. Symbols denote probe measurements in flames A (squares), B (diamonds) and C (triangles). The dashed lines denote flame calculations with GRI-Mech 3.0, and the solid lines are the results of calculations with the increased rate coefficient for $C_2H_2 + OH \rightarrow CH_2CO + H$ discussed in the text.

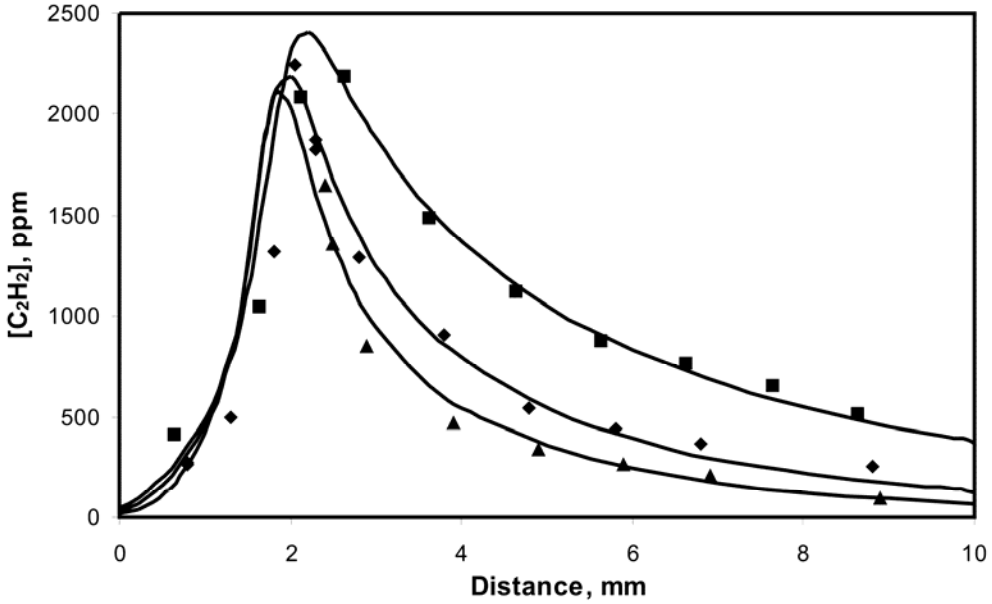

Figure 5.5. Axial profiles of acetylene mole fraction in methane/air flames, φ = 1.45. Symbols denote probe measurements in flames D (squares), E (diamonds) and F (triangles). Solid lines denote flame calculations with the increased rate coefficient for $C_2H_2 + OH \rightarrow CH_2CO + H$ discussed in the text.

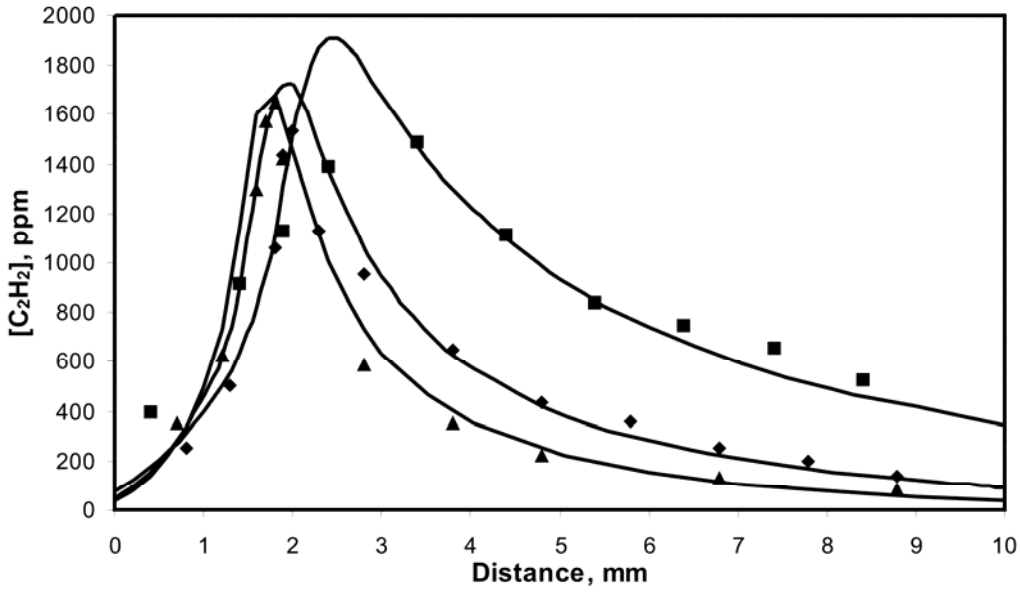

Figure 5.6. Axial profiles of acetylene mole fraction in methane/air flames, φ = 1.40. Symbols denote probe measurements in flames G (squares), H (diamonds) and I (triangles). Solid lines denote flame calculations with the increased rate coefficient for $C_2H_2 + OH \rightarrow CH_2CO + H$ discussed in the text.

In addition, we note substantial discrepancies between the measured acetylene profiles and those obtained from the flame calculations using GRI-Mech 3.0. As can be seen in figure 5.4, the calculations give substantially higher peak concentrations and slower decay in the post-flame zone than those measured, well outside the 20% differences observed between the experimental methods. The computed profiles at the other equivalence ratios showed discrepancies similar to those presented in figure 5.4 This discrepancy has been observed previously [11], where it was attributed to the choice of the rate coefficient of the reaction $C_2H_2 + OH \rightarrow CH_2CO + H$ used in GRI-Mech 3.0. Following the suggestion made in Ref. [11] we increased the pre-exponential factor of the rate coefficient to $1.7 \cdot 10^{12}$ cm^3/mole·s, and these results are also presented in Figs. 5.4-5.6. The calculated acetylene profiles are now in excellent agreement for all flames studied here. Although the limited parameter variation in the present work precludes an unambiguous recommendation regarding increasing the rate coefficient of this reaction, the agreement between experiment and calculations favors this recommendation.

5.4 Conclusions

We report the measurements of acetylene in fuel-rich atmospheric-pressure methane/air flames using spontaneous Raman and extractive probe sampling techniques. Excepting a shift of approximately 1.3 mm, resulting from the acceleration of the combustion products in the probe orifice, the axial Raman and probe profiles are in very good agreement. This result validates using the extractive probe sampling technique as a diagnostic tool for measurements of acetylene for the conditions studied. Substantial disagreement is observed between the experimental profiles of acetylene and those obtained from calculations based on GRI-Mech 3.0, which predict higher acetylene concentrations and slower decay in the post-flame zone. Increasing the pre-exponential factor in the rate coefficient for the reaction $C_2H_2 + OH \rightarrow CH_2CO + H$ to the value of $1.7 \cdot 10^{12}$ cm^3/mole·s brings the calculated acetylene profiles into excellent agreement with those derived experimentally. Further improvement of the sensitivity of both spontaneous Raman and extractive probe techniques will provide more information on acetylene chemistry in fuel-rich methane-air flames. These improvements are currently in progress in our laboratory

Literature

1. J. Warnatz, H. Bockhorn, A. Mozer, H. W. Wenz, *Proc. Combust. Inst.* 19 (1982) 197-209.
2. P. Lindstedt, *Proc. Combust. Inst*. 27 (1998) 269-285.
3. H. Richter, J.B. Howard, *Prog. Energy Combust. Sci.* 26 (4-6) (2000) 565-608.
4. A. Dollet, *Surf. Coat. Technol.* 177 (2004) 245-251.
5. C. P. Fenimore, G. W. Jones, *J. Chem. Phys.* 41 (7) (1964) 1887-1889.
6. J. Vandooren, P. J. van Tiggelen, *Proc. Combust. Inst.* 16 (1977) 1133-1144.
7. D. Bittner, J. B. Howard, *Proc. Combust. Inst.* 19 (1982) 211-221.
8. E. W. Kaiser, *J. Phys. Chem.* 94 (11) (1990) 4493-4499.
9. I. T. Woods, B. S. Haynes, *Combust. Sci. Technol.* 87 (1-6) (1993) 199-215.
10. I. T. Woods, B. S. Haynes, *Proc. Combust. Inst*. 25 (1994) 909.
11. E. W. Kaiser, T. J. Wallington, M. D. Hurley, J. Platz, H. J. Curran, W. J. Pitz, C. K. Westbrook, *J. Phys. Chem. A*. 104 (2000) 8194-8206.
12. J. A. Miller, C. F. Melius, *Proc. Combust. Inst*. 22 (1988) 1031.
13. E. L. Knuth, *Combust. Flame* 103 (3) (1995) 171-180.
14. A. V. Mokhov, S. Gersen, H. B. Levinsky *J. Chem. Phys. Let*., 403 (4-6) (2005) 233-237.
15. A. V. Mokhov, C. E. van der Meij, H. B. Levinsky, *Appl.Opt.* 36 (1997) 3233-3243.
16. G. P. Smith, D. M. Golden, M. Frenklach, N.W. Moriarty, B. Eiteneer, M. Goldenberg, C. T. Bowman, R.K. Hanson, S. Song, W.C. Gardiner, V. Lissanski, Z. Qin, http://www.me.berkeley.edu/gri_mech/.
17. R. J. Cattolica, S. Yoon, E. L. Knuth, *Combust. Sci. Technol.* 28 (5-6) (1982) 225-239.
18. A. T. Hartlieb, B. Atakan, K. Kohse-Hoinghaus, *Combust. Flame* 121 (4) (2000) 610-624.